Positive Oscillating Magnetoresistance in a van der Waals Antiferromagnetic Semiconductor

Lin, Xiaohanwen; Wu, Fan; Ubrig, Nicolas; Liao, Menghan; Yao, Fengrui; Gutierrez Lezama, Ignacio; Morpurgo, Alberto

How to cite

LIN, Xiaohanwen et al. Positive Oscillating Magnetoresistance in a van der Waals Antiferromagnetic Semiconductor. In: Physical review. X, 2025, vol. 15, n° 1, p. 011017. doi: 10.1103/PhysRevX.15.011017

This publication URL: https://archive-ouverte.unige.ch/unige:184566
Publication DOI: 10.1103/PhysRevX.15.011017

Featured in Physics

Positive Oscillating Magnetoresistance in a van der Waals Antiferromagnetic Semiconductor

Xiaohanwen Lin,[*,†] Fan Wu,[†] Nicolas Ubrig, Menghan Liao, Fengrui Yao, Ignacio Gutiérrez-Lezama, and Alberto F. Morpurgo[‡]

Department of Quantum Matter Physics, University of Geneva, 24 Quai Ernest Ansermet, CH-1211 Geneva, Switzerland and Department of Applied Physics, University of Geneva, 24 Quai Ernest Ansermet, CH-1211 Geneva, Switzerland

(Received 25 June 2024; revised 18 October 2024; accepted 5 December 2024; published 30 January 2025)

In all van der Waals layered antiferromagnetic semiconductors investigated so far, a negative magnetoresistance has been observed in vertical transport measurements, with characteristic trends that do not depend on applied bias. Here, we report vertical transport measurements on a layered antiferromagnetic semiconductor $CrPS_4$ that exhibit a drastically different behavior, namely, a strongly bias-dependent, positive magnetoresistance that is accompanied by pronounced oscillations for devices whose thickness is smaller than 10 nm. We establish that this unexpected behavior originates from transport being space-charge limited and not injection limited as for the layered antiferromagnetic semiconductors studied earlier. Our analysis indicates that the positive magnetoresistance and the oscillations only occur when electrons are injected into in-gap defect states, whereas when electrons are injected into the conduction band, the magnetoresistance vanishes. We propose a microscopic explanation for the observed phenomena that combines concepts typical of transport through disordered semiconductors with known properties of the $CrPS_4$ magnetic state, thus capturing all basic experimental observations. Our results illustrate the need to understand, in detail, the nature of transport through vdW magnets in order to extract information about the nature of the order magnetic states and its microscopic properties.

DOI: 10.1103/PhysRevX.15.011017

Subject Areas: Condensed Matter Physics, Electronics, Magnetism

I. INTRODUCTION

In most magnetic systems, the application of an external magnetic field causes a better spin alignment and facilitates electron conduction [1,2]. As a result, the resistance decreases upon the application of a magnetic field [3–12], which is the reason why giant [3] and colossal magnetoresistive systems [5], ferromagnets near the Curie temperature [8], or magnetic tunnel barriers commonly exhibit a negative magnetoresistance [6,10,11]. Indeed, in magnetic conductors, a positive magnetoresistance originating from the coupling of the applied magnetic field to the magnetic state of the materials is only rarely observed [13–15], and when observed, the effect is often relatively small [14,15]. These considerations also hold true for the vast majority of van der Waals (vdW) magnetic materials that have been attracting considerable attention, in which magnetotransport has been investigated either in field-effect transistors or—more commonly—in tunnel barrier devices (i.e., using multilayers of magnetic semiconductors as tunnel barriers) [16–28].

Many of the vdW magnets studied to date are layered antiferromagnetic semiconductors, i.e., materials whose layers are uniformly magnetized with the direction of the magnetization alternating from one layer to the next. Examples of semiconducting layered antiferromagnets include CrI_3 multilayers [18,29], $CrCl_3$ [23], two different allotropes of $CrBr_3$ [30], and CrSBr [31–33]. The vertical transport properties of all of these compounds show distinctive, common characteristics trends. The resistance always decreases upon increasing the applied magnetic field below the spin-flip field; i.e., the magnetoresistance is indeed negative. The decrease of the resistance is monotonous and occurs either through sharp jumps or smoothly, depending on whether magnetic anisotropy is strong or weak. The evolution of the magnetoresistance with magnetic field and temperature is the same irrespective of the voltage applied—as changing the bias only affects the absolute magnitude of the magnetoresistance—and allows

[*]Contact author: Xiaohanwen.Lin@unige.ch
[†]These authors contributed equally to this work.
[‡]Contact author: alberto.morpurgo@unige.ch

mapping the magnetic phase diagram of these systems [16,23,34].

Here, we report vertical transport measurements on multilayers of a layered antiferromagnetic semiconductor $CrPS_4$ that exhibit an unexpected magnetoresistance at odds with the observations that have been reported in all other vdW layered antiferromagnets studied earlier. The evolution of the resistance with magnetic field depends strongly on the applied bias. For small and intermediate bias voltage, the magnetoresistance is large and positive for magnetic field below the spin-flip field, and it becomes negative at larger field. In this bias range, the positive magnetoresistance is accompanied by pronounced magnetoresistance oscillations in devices with thickness below approximately 10 nm. Upon increasing the applied bias, the amplitude of the magnetoresistance and of the oscillations decreases and eventually vanishes. We show that the unexpected observed behavior is rooted in the fact that vertical transport in $CrPS_4$ occurs in the space-charge-limited regime; i.e., transport is not injection limited [see top panel of Fig. 1(a)] as in previously studied layered antiferromagnets. We further show that the different behavior of the magnetoresistance as a function of bias depends on whether space-charge-limited current (SCLC) transport occurs in the trap-limited [see middle panel of Fig. 1(a), (TL-SCLC)] or in the trap-free regime [see bottom panel of Fig. 1(a), (TF-SCLC)]. These conclusions allow us to propose a realistic scenario to explain the unexpected phenomena observed in the experiments in terms of defect-mediated transport processes well established for disordered semiconductors, combined with properties of the magnetic state of $CrPS_4$ multilayers.

II. RESULTS AND ANALYSIS

$CrPS_4$ is a weakly anisotropic layered antiferromagnet, whose easy axis points perpendicular to the layers [35–41]. The material becomes antiferromagnetic below $T_N = 38$ K and exhibits low-temperature spin-flop and spin-flip transitions at approximately 0.8 T and 8 T [27,38,42,43]. The precise values depend on the batch of crystals employed ($CrPS_4$ crystals were purchased from HQ Graphene), as we found that different batches exhibit different doping levels (inferred from the different values of the linear conductivity measured at high temperature). High-quality field-effect transistors based on multilayers have already been reported and have allowed the study of magnetism in the material—as well as its dependence on accumulated charge carrier density—by means of in-plane transport [27,43]. Vertical transport—i.e., transport with current that flows in the direction perpendicular to the layers—has so far been studied only through tetralayer $CrPS_4$, in which direct tunneling gives the dominant contribution to the electrical conductance [44]. The devices that we investigate rely on thicker $CrPS_4$ multilayers (thickness ranging from 4 to 100 nm, with negligible direct tunneling).

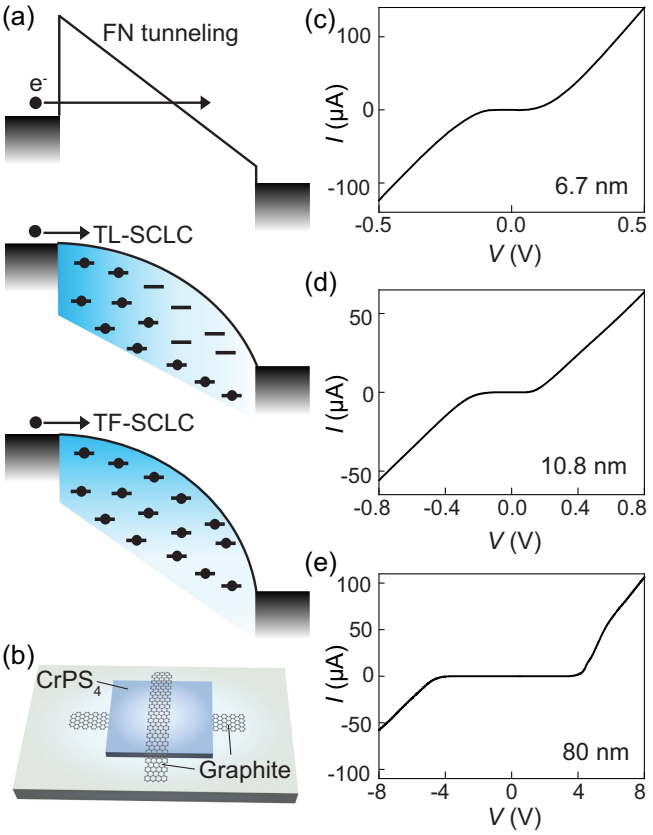

FIG. 1. (a) Cartoon schematics of the band diagrams representative of Fowler-Nordheim tunneling (top panel) and space-charge-limited current, or SCLC (middle and bottom panels), transport. When Fowler-Nordheim tunneling dominates, the applied voltage generates an electric field that tilts the conduction band and increases tunneling probability. The resulting *I*-*V* curves exhibit a very strong exponential dependence of current on bias. In the absence of a sizable barrier at the contacts, transport occurs in the SCLC regime, in which the applied bias both injects electrons in the material and accelerates them. SCLC transport can either be trap limited (middle panel), when the injected electrons propagate through in-gap defect states (traps), or trap-free (bottom panel), when the traps are filled and the largest contribution to the current is due to electrons injected into the conduction band. (b) Schematic representation of our graphite-$CrPS_4$-graphite vertical junctions, which are encapsulated between top and bottom hexagonal-boron nitrate (h-BN) layers (not shown). (c)–(e) Current-voltage (*I*-*V*) characteristics of a 6.7-nm-thick (c), 10.8-nm-thick (d), and 80-nm-thick (e) device measured at 2, 4, and 4 K respectively.

The structures [see Fig. 1(b) for a schematic representation] were assembled in a glove box with a sub-ppm concentration of water and oxygen, and encapsulated between hBN layers. The device realization relies on by-now standard layer exfoliation and manipulation techniques, and it consists of a $CrPS_4$ multilayer in between two multilayer graphene strips attached to the opposite surfaces and acting as contacts [45]. The graphene strips are

contacted by metal electrodes, which are used to interface the structures with the voltage sources and current amplifier employed to measure their I-V characteristics. More details about the device fabrication are presented in the Sec. S1 of the Supplemental Material [46]. A total of ten devices have been investigated, and they show a consistent behavior that we illustrate here by showing data measured on a number of different selected devices.

Figures 1(c)–1(e) show the current-voltage (I-V) characteristics of three devices (with the thickness of the $CrPS_4$ layer ranging from 6.7 nm to 80 nm) measured at low temperature [$T = 2$ K in panel (c); $T = 4$ K in panels (d) and (e)]. The I-V curves exhibit a clear nonlinearity, which is nevertheless much less pronounced as compared to most layered antiferromagnetic semiconductors studied earlier [18,20,47], in which the current increases exponentially fast with bias. To appreciate the difference, we analyze the I-V characteristics by plotting them in a double-logarithmic scale [see Figs. 2(a)–2(f), as well as Fig. S3 in Ref. [46]]. The double-logarithmic plot shows the presence of multiple regimes with the current depending differently on voltage [Figs. 2(d)–2(f), as well as Fig. S3 in Ref. [46]]. In the lowest voltage range—i.e., between 1 and 10 mV—I is either linear in V or too small to be measured (i.e., for thicker multilayers, the current is below the sensitivity of our amplifiers). For larger voltages, I increase very rapidly with increasing V, compatibly with a power law $I \propto V^m$ with very large power ($m \approx 10$). Eventually, the double-logarithmic plot tends to flatten, resulting in a $I \propto V^2$ dependence [see the zoomed-in plots in Figs. 2(a) and 2(c), and Fig. S3 in Ref. [46] for data from additional devices showing that $I \propto V^2$ at high bias].

In a minority of cases, the power of the $I \propto V^m$ relation decreases below 2 at the highest bias, and the I-V relation tends to approach linearity [as visible, for instance, in Fig. 2(b)]. This happens when the series resistance of the graphene strip used as an electrode—larger than 10 kΩ for the longest contact strips employed in the device fabrication—cannot be neglected. To illustrate the role of the series resistance, we look at one of the devices that we investigated, in which multiterminal measurements could be made to compare the resistance value measured with and without the contribution of the resistance of the graphene strip (in a four-terminal configuration, we measure only the voltage drop across the $CrPS_4$ multilayer). Data from this device are shown in Fig. S4 of Ref. [46]. It is clear that at high bias, the slope of the I-V curve decreases below 2 for measurements made in a two-terminal configuration (i.e., when the resistance includes the series resistance of the graphene strip used as an electrode), but the curve is perfectly quadratic when measured in a four-terminal configuration (to exclude the series resistance and probe exclusively vertical transport through the $CrPS_4$ multilayer).

Finding that at high bias the I-V characteristic of the $CrPS_4$ multilayers becomes quadratic provides a first, clear indication that, at low temperature, vertical transport through $CrPS_4$ multilayers occurs in the so-called SCLC [48,49] regime. This transport mechanism is different from that observed in similar structures that probe vertical

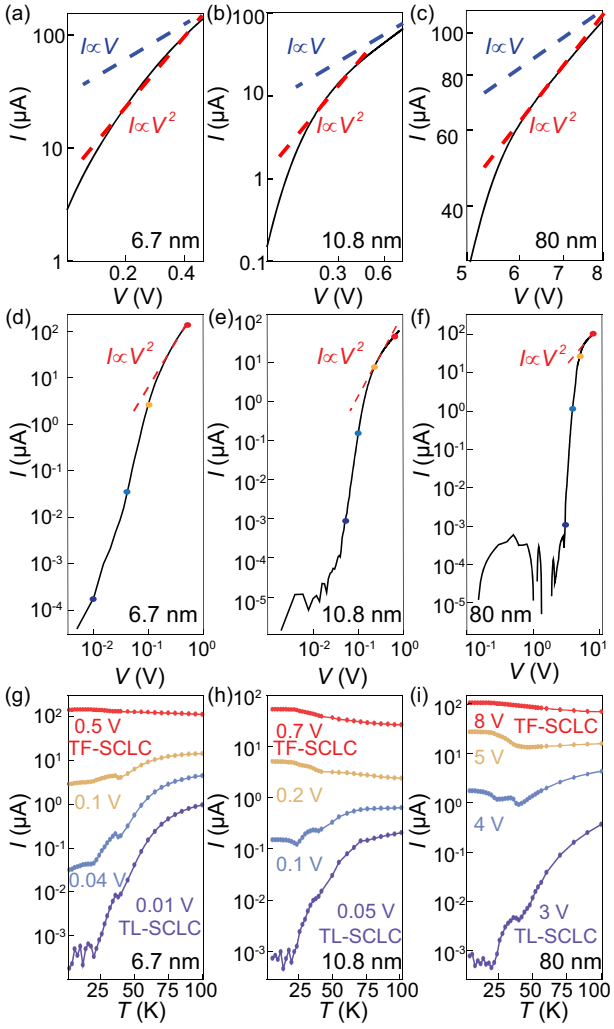

FIG. 2. (a)–(f) Double-logarithmic plots of the I-V characteristics shown in Figs. 1(c)–1(e) [(a), (d) 6.7-nm device; (b), (e) 10.8-nm device; (c), (f) 80-nm device). Panels (a)–(c) are zoom-ins of the high-voltage bias parts of the I-V curves. The red (slope2) and blue (slope1) dashed lines are guides for the eye. In panels (a) and (c), the red dashed line overlaps with the data at high bias (i.e., $I \propto V^2$). In panel (b), the slope at high bias is smaller than 2 and seems to approach 1 as V is increased due to the series resistance of the long graphene strip used as the contact (see discussion in the main text and Fig. S4 in Ref. [46] for a comparison of two- and four-terminal measurements on another device, illustrating the effects of the contact resistance). (g)–(i) Temperature dependence of the current measured at different biases for the three devices whose I-V curves are shown in panels (d)–(f) [see legend for device thickness; purple, blue, yellow, and red curves represent measurements taken at biases corresponding to the dots of the same color in panels (d)–(f)]. At low bias, the devices exhibit an insulating behavior (the current decreases with decreasing T), whereas at sufficiently high bias, the behavior is metallic (the current increases with increasing T).

transport in other layered antiferromagnetic semiconductors studied earlier. When transport is mediated by SCLC, the role of the applied bias is twofold: It injects charge carriers into the material (just like when charging a capacitor), and it accelerates them. Different regimes of space-charge-limited transport are realized depending on whether the charge is injected into in-gap localized states associated with defects (traps) or into states inside a band [48,49]. In the first case—referred to as trap-limited SCLC—the current decreases with lowering temperature and eventually saturates at low T, when electron motion is mediated by elastic hopping processes. In the second case—referred to as trap-free SCLC—the current increases upon cooling since, for electrons occupying states in a band, the mobility is normally larger at lower T. Thus, to confirm that what we observe in our measurements is effectively space-charge-limited transport, we look at the evolution of the current with temperature at different values of the applied bias V.

Figures 2(g)–2(i) show the temperature dependence of the current measured for four values of applied voltage, spanning across the different regimes observed in the double-logarithmic plot of the I-V characteristics. It is apparent that at low bias, the current I decreases rapidly upon lowering T—a behavior typical of thermally-activated or variable-range hopping. As the applied bias is increased, the current still decreases upon cooling but eventually tends to saturate at low temperature to a value that is sufficiently large to be detected. Such a temperature-independent transport regime is expected when transport is mediated by elastic hopping. At sufficiently large bias, the current increases upon lowering temperature. Such a behavior, indicative of band transport, starts to occur as the applied bias is such that the I-V curve in the double-logarithmic plot enters the $I \propto V^2$ regime. Microscopically, band transport occurs when the nonequilibrium electron distribution generated by the applied bias, and commonly described by a so-called quasi Fermi level, results in a sizable population of states in the conduction band. Therefore, overall, the evolution of the current with temperature that we observe experimentally is precisely the one expected for SCLC, passing from the trap-limited transport regime (in the bias range where the current decreases upon decreasing T) to the trap-free regime at high bias (where electrons injected in the conduction band dominate the current flow). It is therefore the concomitant observation of a high-bias $I \propto V^2$ regime, and of the correlation between bias and temperature dependence of the current, that allows us to conclude that vertical transport occurs in the SCLC regime, irrespective of the multilayer thickness (at least in the thickness range investigated).

The behavior of the magnetoresistance of van der Waals magnetic semiconductors operating in the SCLC regime has never been reported and is currently unknown. We find that at small and intermediate bias, the resistance exhibits a pronounced increase corresponding to a positive magnetoresistance between 1000% and 2000%, before eventually decreasing as H approaches the spin-flip field $\mu_0 H_{\text{flip}} \simeq 8$ T [see Figs. 3(a)–3(c)]. For $H > H_{\text{flip}}$, the resistance is lower than at $\mu_0 H = 0$ T; i.e., the high-field magnetoresistance is negative (with a typical magnitude of approximately 100%). In devices with thickness smaller than approximately 10 nm, the positive magnetoresistance observed for $H < H_{\text{flip}}$ exhibits pronounced oscillations. In thick devices, these oscillations are either absent or cannot be clearly resolved and only result in less-pronounced features (e.g., magnetoresistance "kinks"). Such pronounced magnetoresistance oscillations have never been observed in any vdW magnetic semiconductor.

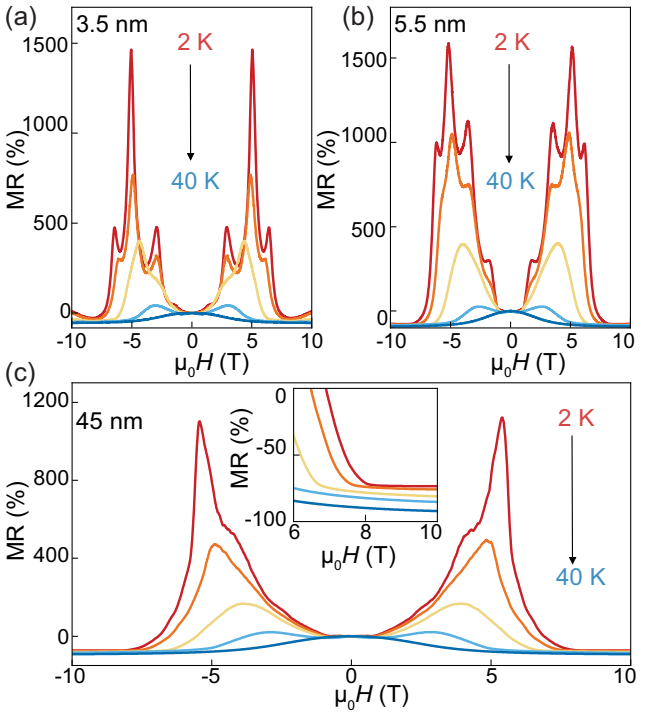

FIG. 3. (a)–(c) Temperature dependence of the magnetoresistance $\text{MR} = [R(H) - R(0)/R(0)]$ measured at low bias (in the TL SCLC regime) on three different devices with a $CrPS_4$ layer that is 3.5 (a), 5.5 (b), and 45 nm (c) thick (the magnetic field is applied perpendicular to the layers). Red, orange, yellow, and light and dark blue solid lines represent magnetoresistance measured at $T = 2$, 10, 20, 30, and 40 K, respectively. In all our devices, a large (up to 1000%–2000% at the lowest temperatures) positive magnetoresistance is observed below the spin-flip field (≃8 T), and it exhibits pronounced oscillations in devices that are less than 10 nm thick. The magnetoresistance becomes negative and smaller [approximately 100%, see inset of panel (c)] when the field applied is larger than the spin-flip field.

Upon increasing temperature, the magnetoresistance decreases, and for $T > T_N$—in the paramagnetic state—only a weak and broad negative magnetoresistance persists [see Figs. 3(a)–3(c)]. The overall evolution as a function of temperature and magnetic field is illustrated in detail in

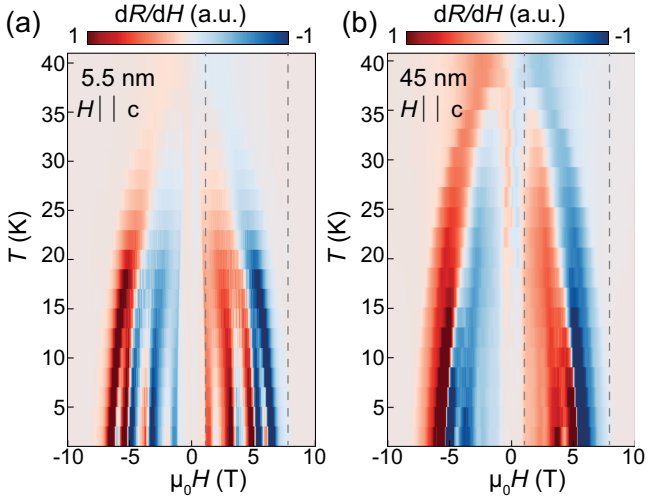

FIG. 4. (a), (b) Color plots of dR/dH calculated from the conductance $R(H,T)$ measured on the 5.5-nm-thick (a) and 45-nm-thick (b) devices whose magnetoresistance data are shown in Figs. 3(b) and 3(c), respectively. In all devices, the dR/dH plot clearly shows the spin-flop and spin-flip fields, which shift towards lower values as T increases up to the critical temperature $T_N \sim 38$ K. The maxima and minima of the oscillations seen in sufficiently thin devices [panel (a)] appear as fringes in the color plot, which also move towards lower field values as T is increased (i.e., they evolve with T as H_{flip} does). The dashed vertical lines in the panels represent the spin-flop (≃0.8 T) and the spin-flip (≃8 T) transitions observed at the lowest temperature.

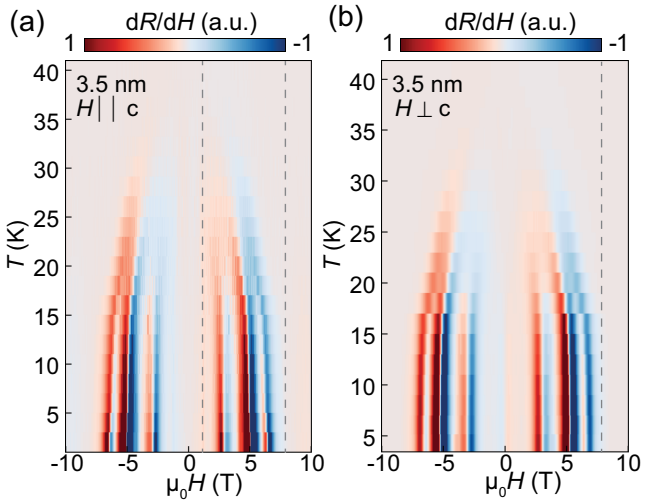

FIG. 5. Color plot of dR/dH as a function of temperature T and magnetic field H measured on a device realized on a 3.5-nm-thick $CrPS_4$ multilayer. The data in panels (a) and (b) have been measured with the field parallel or perpendicular to the c axis, respectively. The dashed vertical lines in the panels represent the spin-flop (≃0.8 T) and the spin-flip (≃8 T) transitions observed at the lowest temperature.

Fig. 4 with color plots of $dR/dH(H,T)$. The data clearly show how H_{flop} and H_{flip} shift to lower values at higher T and eventually vanish at the Néel temperature $T_N \sim 38$ K, as expected. Interestingly, the data further show that magnetoresistance oscillations also evolve with increasing temperature as the spin-flip field does. This result is unexpected because it is well established that, in bulk $CrPS_4$ crystals, no magnetic transition occurs at the corresponding magnetic field values [27,38].

We find that the overall behavior of the magnetoresistance is nearly identical when the magnetic field is applied perpendicular or parallel to the plane [see Figs. 5(a) and 5(b), as well as Fig. S5 in Ref. [46]]. This finding is the case for the complete magnetic field dependence and for its temperature evolution. Indeed, virtually all features observed in the magnetoresistance are present irrespective of whether the field is applied in plane or perpendicular to the plane (with the exception of features originating from the spin-flop transition, which are seen when the field is applied perpendicular to the layers, as expected). These observations indicate that the magnetic field strongly influences the electron motion by coupling to the magnetic spin structure.

The magnetoresistance also decreases rapidly upon increasing bias. This result is shown in Fig. 6 for two devices based on one of the thinnest [Fig. 6(a)] and one of the thickest [Fig. 6(b)] $CrPS_4$ multilayers studied. It can be seen by comparing the data in Fig. 6(b) with the I-V curves for the same devices shown in Fig. 2(c) that the bias at

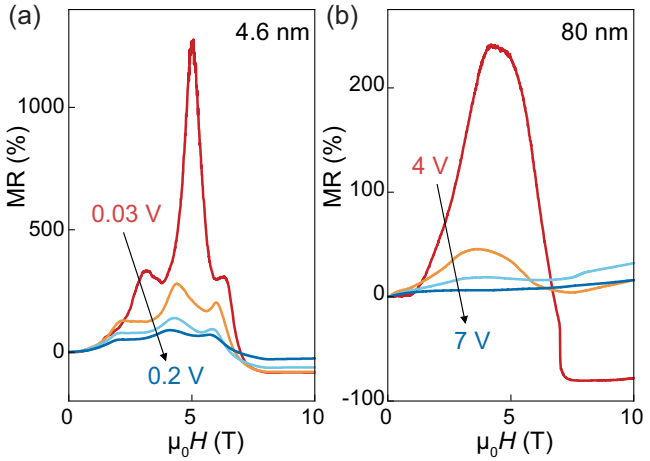

FIG. 6. (a), (b) Bias dependence of the magnetoresistance measured in a 4.6-nm-thick (a) and an 80-nm-thick (b) device. The red, orange, and light and dark blue solid lines represent the magnetoresistance measured at 0.03 (4), 0.06 (5), 0.12 (6), and 0.2 (7) V in panel (a) [(b)]. The magnetoresistance is large at low bias and decreases with increasing bias, eventually vanishing when entering the TF-SCLC regime (a small magnetoresistance persists in some devices either because the applied bias is not enough to go deeply in the TF-SCLC regime or because a small contribution from the magnetoresistance of the graphene contacts becomes visible at sufficiently high bias).

which the magnetoresistance disappears corresponds to the onset of the high-voltage range over which $I \propto V^2$ (a similar observation has been made on other devices as well). This finding implies that, in the trap-free limit of the SCLC regime, when current is carried by electrons injected in the conduction band of $CrPS_4$, virtually no magnetoresistance is observed, neither positive for $H < H_{\mathrm{flip}}$ nor negative for $H > H_{\mathrm{flip}}$. Indeed, in all devices investigated in which a bias sufficient to enter the trap-free limit was applied, no sizable magnetoresistance was found to survive. At the highest bias, when the resistance is in the 10-kΩ range, a small positive magnetoresistance due to the contribution of graphene is visible in some devices, consistently with the fact—mentioned earlier—that in some devices at the highest bias, transport is limited by the resistance of the graphene strip acting as the contact. Finding that the magnetoresistance tends to vanish when the applied bias V brings the device into the $I \propto V^2$ regime allows us to conclude that the magnetoresistance (as well as the magnetoresistance oscillations) originates from electrons propagating via localized defect states inside the gap of $CrPS_4$.

Establishing that the positive magnetoresistance originates from electrons hopping between localized states is important because, in conventional (i.e., nonmagnetic) semiconductors, a positive magnetoresistance in the hopping regime can be readily explained in terms of wave-function squeezing induced by the applied magnetic field. The orbital effect of the magnetic field on states localized at defects enhances confinement and decreases the spatial extension of the wave functions. As a result, the overlap of the wave functions located at neighboring hopping sites decreases, as does the corresponding hopping probability [50]. Since at low temperature the distance of the impurities hosting states with the same energy (i.e., the states that mediate elastic hopping transport) is large, the wave-function overlap is due to the wave-function tail, whose amplitude decreases exponentially with applied magnetic field. In this regime, theory predicts a positive magnetoresistance given by $R(H)/R(H=0) = e^{\alpha H^2}$ [50], such that

$$\ln(R(H)/R(H=0)) = \alpha H^2. \tag{1}$$

Indeed, if we plot the logarithm of $R(H)/R(H=0)$ versus H^2 for devices based on $CrPS_4$ layers of thickness between 3 and 80 nm, we always find a linear relation for values of $\mu_0 H$ up to approximately 3 Tesla [Fig. 7(a)].

For nonmagnetic semiconductors, the magnetoresistance at sufficiently high magnetic field eventually saturates, but for a layered antiferromagnet such as $CrPS_4$, the situation is different. In a layered antiferromagnetic semiconductor, increasing the applied magnetic field not only decreases the extension of the localized states but also causes the magnetization of adjacent layers to cant in the same direction. This finding is important because when the magnetization in adjacent layers points in opposite directions (for $\mu_0 H = 0$ T), electrons cannot hop from one layer to the next because the exchange energy is too large (approximately 0.6 eV in $CrPS_4$ [43]). Electrons then need to hop to defect states located in the next-next layer so that the overlap of the initial and final states involved in the hopping process is truly due to the tail of the wave function, and the mechanism for positive magnetoresistance discussed above is pertinent.

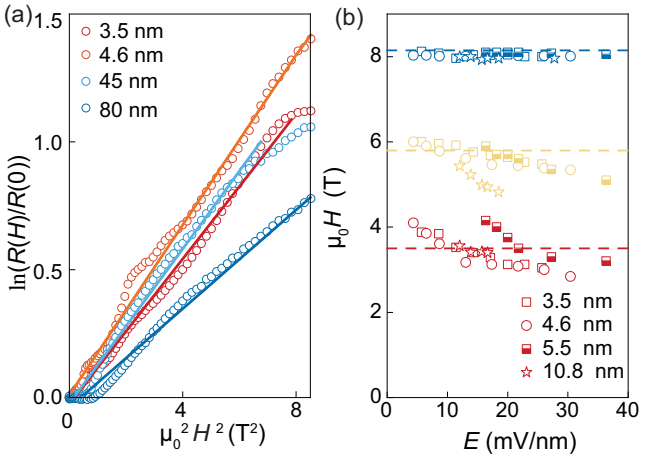

FIG. 7. (a) Plot of $\ln(R(H)/R(H=0))$ as a function of H^2 (with field applied perpendicular to the layers) measured in several different devices (with the $CrPS_4$ layer, respectively, 3.5, 4.6, 45, and 80 nm thick). The linear dependence indicates that the positive magnetoresistance measured in the TL-SCLC regime is due to squeezing of the wave functions of the states involved in the hopping process. (b) Magnetic field values of the two local minima associated with the magnetoresistance oscillations observed in devices thinner than 10 nm (data taken at 2 K or 4 K, depending on the device; the thickness of the $CrPS_4$ layer is indicated in the legend). The red, yellow, and blue data points correspond to the first minimum in the oscillations, the second minimum, and the spin-flip field. The dashed lines represent the value of the spin-flip field extracted from $CrPS_4$ transistor measurements done on $CrPS_4$ bilayers (red dashed line), trilayers (yellow dashed line), and thick, bulklike multilayers (blue dashed line) [51].

As the magnetic field is increased and the magnetization in different layers cant towards the field direction, however, defect states in adjacent layers have a larger parallel spin component. The parallel spin component increases the probability for electrons to hop from states in one layer to states in the neighboring layer. Increasing spin canting, therefore, effectively reduces the distance between states involved in the electron hopping process and eventually causes the magnetoresistance to start deceasing at sufficiently large magnetic field. Thus, the observed magnetoresistance in $CrPS_4$ devices peaks below the spin-flip field. Eventually, for H above the spin-flip field, the magnetization of all layers points in the same direction, and hopping is fully dominated by states in the neighboring

layers, which have a much larger overlap. The closer distance between the defect states means that the wave-function overlap is not determined by their exponential tails and is therefore no longer exponentially sensitive to an increase in magnetic field. In this regime, magnetotransport is likely dominated by a different process, namely, the shift to a lower energy of the conduction band edge that has recently been observed in field-effect transistor measurements [42,43]. The lowering of the conduction band edge increases the spatial extension of the localized wave functions relative to the $\mu_0 H = 0$ T case, resulting in a negative magnetoresistance for $H > H_{\text{flip}}$.

The experimental observations indicate that the role played by spin canting in adjacent layers to determine the relevant hopping processes is likely also the reason for the magnetoresistance oscillations observed in sufficiently thin $CrPS_4$ layers. This idea is suggested by the analysis of the magnetic field at which the resistance exhibits minima in devices thinner than approximately 10 nm. The position of these magnetoresistance minima (as a function of applied electric field) is summarized in Fig. 7(b), based on data measured on four different devices with thickness smaller than 10 nm. We focus on the minima that are clearly defined so that their position can be determined unambiguously (more shoulders or kinks become visible as the $CrPS_4$ thickness increases, but the positions of those features are more difficult to determined precisely). In all devices, we find two such minima, at $\mu_0 H \simeq 3.5$–4 T and $\mu_0 H \simeq 6$ T. We also plot the value of the spin-flip field $\mu_0 H \simeq 8$ T, at which the magnetoresistance saturates to a constant value. Interestingly, the values of $\mu_0 H$ for the two minima identified match quite precisely the spin-flip field of bilayer and trilayer $CrPS_4$, which we know from separate studies of MR on $CrPS_4$ field-effect transistors [51]. This observation suggests that, inside the multilayers used to study vertical transport, structural domains are present, with stacking faults that magnetically decouple the $CrPS_4$ layers.

Structural defects (such as stacking faults) can cause electronic decoupling of thin layers within thicker crystals, resulting in $CrPS_4$ regions that effectively behave as bi-, tri-, and tetralayers. In terms of their magnetic response, these layers would have a correspondingly lower spin-flip field, as expected theoretically. For bilayers, for instance, the spin-flip field is half that of the bulk because each constituent layer feels the exchange interaction of only one other neighboring layer and not of two like in the bulk (for a study of the spin-flip field as a function of multilayer thickness in low-anisotropy layered antiferromagnets, see past work on $CrCl_3$ [23]). We therefore suggest that the observed peaks in the magnetoresistance originate from the contributions of regions inside the device in which stacking faults cause electronic decoupling of a few layers, which contribute to the total measured resistance. Specifically, because of the lower spin-flip field, in these regions, a large spin canting starts at smaller H, causing their contribution to the total magnetoresistance to also peak at values of H smaller than that of thick multilayers. To confirm this idea —and explore whether electronic decoupling caused by structural defects may be controlled to engineer the magnetoresistive response—it would certainly be interesting to investigate crystals of different structural quality.

III. CONCLUSIONS

In devices based on vdW layered antiferromagnetic semiconductors studied in the past, transport was virtually always injection limited, and the experimental results were properly captured in terms of a phenomenological Fowler-Nordheim tunneling description [52,53]. This same approach, however, does not properly describe the behavior of $CrPS_4$-based devices because vertical transport in $CrPS_4$ occurs in the space-charge-limited current regime; i.e., electron injection at the contacts is not the process limiting current flow. Why vertical transport occurs in the SCLC regime in $CrPS_4$ multilayers (whereas for all other 2D magnetic materials studied earlier at high bias, transport was found to be injection limited) remains to be understood in detail. It is probably due to the high (unintentional) doping level of $CrPS_4$ crystals, which shifts the Fermi level in the material much closer to the conduction band edge as compared to other 2D magnetic van der Waals semiconductors. The closer proximity of the Fermi level to the conduction band edge is corroborated by the observation of a linear transport regime in many of our devices down to low temperature, with relatively small activation energy of the resistance (30 to 40 meV depending on crystals, see Fig. S2 in Ref. [46]), much smaller than, for instance, in CrI_3 (where the activation energy is approximately 200 meV) [16]. The proximity of the Fermi level to the conduction band edge enhances both the density of states at the Fermi level and the overlap of the wave functions of electrons localized at defects, drastically increasing conductivity due to in-gap states through $CrPS_4$. The conductivity due to the in-gap state implies that charge injected in the material is sufficiently mobile to enable the observation of current, which is precisely the idea of space-charge-limited transport. In other vdW magnets, in contrast, charge injected into in-gap states inside the material does not lead to any measurable current because the much larger distance between the Fermi level and conduction band edge implies that electrons in defects are much more strongly localized. As a consequence, current is only observed when the bias is large enough to directly inject electrons into the band, which is the idea behind Fowler-Nordheim tunneling.

Irrespective of the precise microscopic reason why vertical transport in $CrPS_4$ is space-charge limited, what is particularly interesting is that the SCLC transport regime has not been investigated earlier in layered vdW magnets,

and nothing is known about the expected behavior of the magnetoresistance. In the space-charge-limited transport regime, the applied bias accumulates electrons in the material—similarly to what happens in a capacitor—and it then accelerates them. At low bias, electrons are injected into localized states and can propagate only via hopping. Upon increasing the bias, the larger density of accumulated electrons also starts to occupy states in the conduction band. Electrons occupying these states can propagate much more easily and cause a large decrease in resistance. The microscopic processes responsible for current flow are therefore different at low and high bias. This difference is the reason for the strong bias dependence of the magnetoresistive response and of the temperature dependence of the measured resistance. Because $CrPS_4$ devices are the first in the family of vdW semiconducting magnets to operate in the space-charge-limited transport regime, their behavior is different from that observed in materials studied earlier and appears anomalous at first sight.

Our work succeeds in rationalizing all the seemingly anomalous experimental observations by considering the interplay between semiconductor physics—which determines how the localized states responsible for hopping respond to an applied magnetic field—with the evolution of the magnetic state of $CrPS_4$ upon increasing the applied magnetic field—which determines whether electrons can or cannot hop to states in an adjacent layer. The application of the magnetic field enhances localization effects of electrons in in-gap states involved in the hopping conduction, causing the resistance to increase at low field. The gradual increase in canting of the magnetization of different layers in the same direction enhances the probability for electrons to hop from one layer to the nearest neighboring one, which effectively decreases the distance between hopping sites. The net result is the positive and nonmonotonic magnetoresistance that we observe. Once the accumulated electrons populate states in the band, the resistance becomes much less sensitive to the magnetic field. The observed overall decrease in resistance relative to the value measured at $\mu_0 H = 0$ T is again likely due to the downshift of the conduction band edge.

In summary, our results show how vertical magnetoresistance measurements on van der Waals semiconducting magnets can exhibit a very different evolution with field, temperature, and bias in different materials with virtually identical magnetic states, simply because of the different regimes in which transport occurs. Our experiments also reveal the behavior of the magnetoresistance in the space-charge-limited transport regime, that in van der Waals semiconducting magnets have never been investigated. Both these issues are important to realize magnetoresistance measurements as a reliable technique to investigate the magnetic properties of atomically thin van der Waals magnets.

ACKNOWLEDGMENTS

The authors gratefully acknowledge Alexandre Ferreira for continuous and valuable technical support, and M. Gibertini, J. Fernandez-Rosier, and I. Martin for interesting discussions. A. F. M. acknowledges financial support from the Swiss National Science Foundation Division II under Project No. 200021-219424.

[1] I. Žutić, J. Fabian, and S. Das Sarma, *Spintronics: Fundamentals and applications*, Rev. Mod. Phys. **76**, 323 (2004).
[2] A. Fert, *Nobel lecture: Origin, development, and future of spintronics*, Rev. Mod. Phys. **80**, 1517 (2008).
[3] M. N. Baibich, J. M. Broto, A. Fert, F. N. Van Dau, F. Petroff, P. Etienne, G. Creuzet, A. Friederich, and J. Chazelas, *Giant magnetoresistance of* (001)Fe/(001)Cr *magnetic superlattices*, Phys. Rev. Lett. **61**, 2472 (1988).
[4] S. S. P. Parkin, N. More, and K. P. Roche, *Oscillations in exchange coupling and magnetoresistance in metallic superlattice structures:* Co/Ru*,* Co/Cr*, and* Fe/Cr, Phys. Rev. Lett. **64**, 2304 (1990).
[5] S. Jin, T. H. Tiefel, M. McCormack, R. A. Fastnacht, R. Ramesh, and L. H. Chen, *Thousandfold change in resistivity in magnetoresistive* La − Ca − Mn − *O films*, Science **264**, 413 (1994).
[6] J. S. Moodera, L. R. Kinder, T. M. Wong, and R. Meservey, *Large magnetoresistance at room temperature in ferromagnetic thin film tunnel junctions*, Phys. Rev. Lett. **74**, 3273 (1995).
[7] C. N. R. Rao, A. K. Cheetham, and R. Mahesh, *Giant magnetoresistance and related properties of rare-earth manganates and other oxide systems*, Chem. Mater. **8**, 2421 (1996).
[8] A. P. Ramirez, R. J. Cava, and J. Krajewski, *Colossal magnetoresistance in* Cr*-based chalcogenide spinels*, Nature (London) **386**, 156 (1997).
[9] A. Gupta and J. Sun, *Spin-polarized transport and magnetoresistance in magnetic oxides*, J. Magn. Magn. Mater. **200**, 24 (1999).
[10] S. S. Parkin, C. Kaiser, A. Panchula, P. M. Rice, B. Hughes, M. Samant, and S.-H. Yang, *Giant tunnelling magnetoresistance at room temperature with* MgO *(100) tunnel barriers*, Nat. Mater. **3**, 862 (2004).
[11] S. Yuasa, T. Nagahama, A. Fukushima, Y. Suzuki, and K. Ando, *Giant room-temperature magnetoresistance in single-crystal* Fe/MgO/Fe *magnetic tunnel junctions*, Nat. Mater. **3**, 868 (2004).
[12] M. Gajek, M. Bibes, S. Fusil, K. Bouzehouane, J. Fontcuberta, A. Barthélémy, and A. Fert, *Tunnel junctions with multiferroic barriers*, Nat. Mater. **6**, 296 (2007).
[13] C. Tan, M. Deng, Y. Yang, L. An, W. Ge, S. Albarakati, M. Panahandeh-Fard, J. Partridge, D. Culcer, B. Lei, T. Wu, X. Zhu, M. Tian, X. Chen, R.-Q. Wang, and L. Wang, *Electrically tunable, rapid spin–orbit torque induced modulation of colossal magnetoresistance in* $Mn_3Si_2Te_6$ *nanoflakes*, Nano Lett. **24**, 4158 (2024).
[14] G. Long, H. Henck, M. Gibertini, D. Dumcenco, Z. Wang, T. Taniguchi, K. Watanabe, E. Giannini, and

A. F. Morpurgo, *Persistence of magnetism in atomically thin* $MnPS_3$ *crystals*, Nano Lett. **20**, 2452 (2020).

[15] N. Manyala, Y. Sidis, J. F. DiTusa, G. Aeppli, D. P. Young, and Z. Fisk, *Addendum: Magnetoresistance from quantum interference effects in ferromagnets*, Nature (London) **408**, 616 (2000).

[16] Z. Wang, I. Gutiérrez-Lezama, N. Ubrig, M. Kroner, M. Gibertini, T. Taniguchi, K. Watanabe, A. Imamoglu, E. Giannini, and A. F. Morpurgo, *Very large tunneling magnetoresistance in layered magnetic semiconductor* CrI_3, Nat. Commun. **9**, 2516 (2018).

[17] D. R. Klein, D. MacNeill, J. L. Lado, D. Soriano, E. Navarro-Moratalla, K. Watanabe, T. Taniguchi, S. Manni, P. Canfield, J. Fernández-Rossier, and P. Jarillo-Herrero, *Probing magnetism in 2D van der Waals crystalline insulators via electron tunneling*, Science **360**, 1218 (2018).

[18] T. Song, X. Cai, M. W.-Y. Tu, X. Zhang, B. Huang, N. P. Wilson, K. L. Seyler, L. Zhu, T. Taniguchi, K. Watanabe, M. A. McGuire, D. H. Cobden, D. Xiao, W. Yao, and X. Xu, *Giant tunneling magnetoresistance in spin-filter van der Waals heterostructures*, Science **360**, 1214 (2018).

[19] H. H. Kim, B. Yang, T. Patel, F. Sfigakis, C. Li, S. Tian, H. Lei, and A. W. Tsen, *One million percent tunnel magnetoresistance in a magnetic van der Waals heterostructure*, Nano Lett. **18**, 4885 (2018).

[20] Z. Wang, T. Zhang, M. Ding, B. Dong, Y. Li, M. Chen, X. Li, J. Huang, H. Wang, X. Zhao, Y. Li, D. Li, C. Jia, L. Sun, H. Guo, Y. Ye, D. Sun, Y. Chen, T. Yang, J. Zhang, S. Ono, Z. Han, and Z. Zhang, *Electric-field control of magnetism in a few-layered van der Waals ferromagnetic semiconductor*, Nat. Nanotechnol. **13**, 554 (2018).

[21] D. R. Klein, D. MacNeill, Q. Song, D. T. Larson, S. Fang, M. Xu, R. A. Ribeiro, P. C. Canfield, E. Kaxiras, R. Comin, and P. Jarillo-Herrero, *Enhancement of interlayer exchange in an ultrathin two-dimensional magnet*, Nat. Phys. **15**, 1255 (2019).

[22] T. Song, Z. Fei, M. Yankowitz, Z. Lin, Q. Jiang, K. Hwangbo, Q. Zhang, B. Sun, T. Taniguchi, K. Watanabe, M. A. McGuire, D. Graf, T. Cao, J.-H. Chu, D. H. Cobden, C. R. Dean, D. Xiao, and X. Xu, *Switching 2D magnetic states via pressure tuning of layer stacking*, Nat. Mater. **18**, 1298 (2019).

[23] Z. Wang, M. Gibertini, D. Dumcenco, T. Taniguchi, K. Watanabe, E. Giannini, and A. F. Morpurgo, *Determining the phase diagram of atomically thin layered antiferromagnet* $CrCl_3$, Nat. Nanotechnol. **14**, 1116 (2019).

[24] G. Long, H. Henck, M. Gibertini, D. Dumcenco, Z. Wang, T. Taniguchi, K. Watanabe, E. Giannini, and A. F. Morpurgo, *Persistence of magnetism in atomically thin* $MnPS_3$ *crystals*, Nano Lett. **20**, 2452 (2020).

[25] E. J. Telford, A. H. Dismukes, K. Lee, M. Cheng, A. Wieteska, A. K. Bartholomew, Y. Chen, X. Xu, A. N. Pasupathy, X. Zhu, C. R. Dean, and X. Roy, *Layered antiferromagnetism induces large negative magnetoresistance in the van der Waals semiconductor* CrSBr, Adv. Mater. **32**, 2003240 (2020).

[26] F. Wu, I. Gutiérrez-Lezama, S. A. López-Paz, M. Gibertini, K. Watanabe, T. Taniguchi, F. O. von Rohr, N. Ubrig, and A. F. Morpurgo, *Quasi-1D electronic transport in a 2D magnetic semiconductor*, Adv. Mater. **34**, 2109759 (2022).

[27] R. Wu, A. Ross, S. Ding, Y. Peng, F. He, Y. Ren, R. Lebrun, Y. Wu, Z. Wang, J. Yang, A. Brataas, and M. Kläui, *Magnetotransport study of van der Waals* $CrPS_4/(Pt, Pd)$ *heterostructures: Spin-flop transition and room-temperature anomalous Hall effect*, Phys. Rev. Appl. **17**, 064038 (2022).

[28] F. Yao, V. Multian, Z. Wang, N. Ubrig, J. Teyssier, F. Wu, E. Giannini, M. Gibertini, I. Gutiérrez-Lezama, and A. F. Morpurgo, *Multiple antiferromagnetic phases and magnetic anisotropy in exfoliated* $CrBr_3$ *multilayers*, Nat. Commun. **14**, 4969 (2023).

[29] B. Huang, G. Clark, E. Navarro-Moratalla, D. R. Klein, R. Cheng, K. L. Seyler, D. Zhong, E. Schmidgall, M. A. McGuire, D. H. Cobden, W. Yao, D. Xiao, P. Jarillo-Herrero, and X. Xu, *Layer-dependent ferromagnetism in a van der Waals crystal down to the monolayer limit*, Nature (London) **546**, 270 (2017).

[30] Z. Wang, I. Gutiérrez-Lezama, D. Dumcenco, N. Ubrig, T. Taniguchi, K. Watanabe, E. Giannini, M. Gibertini, and A. F. Morpurgo, *Magnetization dependent tunneling conductance of ferromagnetic barriers*, Nat. Commun. **12**, 6659 (2021).

[31] E. J. Telford, A. H. Dismukes, K. Lee, M. Cheng, A. Wieteska, A. K. Bartholomew, Y.-S. Chen, X. Xu, A. N. Pasupathy, X. Zhu, C. R. Dean, and X. Roy, *Layered antiferromagnetism induces large negative magnetoresistance in the van der Waals semiconductor* CrSBr, Adv. Mater. **32**, 2003240 (2020).

[32] C. Ye, C. Wang, Q. Wu, S. Liu, J. Zhou, G. Wang, A. Söll, Z. Sofer, M. Yue, X. Liu, M. Tian, Q. Xiong, W. Ji, and X. Renshaw Wang, *Layer-dependent interlayer antiferromagnetic spin reorientation in air-stable semiconductor* CrSBr, ACS Nano **16**, 11876 (2022).

[33] X. Lin, F. Wu, S. A. López-Paz, F. O. von Rohr, M. Gibertini, I. Gutiérrez-Lezama, and A. F. Morpurgo, *Influence of magnetism on vertical hopping transport in* CrSBr, Phys. Rev. Res. **6**, 013185 (2024).

[34] D. Soler-Delgado, F. Yao, D. Dumcenco, E. Giannini, J. Li, C. A. Occhialini, R. Comin, N. Ubrig, and A. F. Morpurgo, *Probing magnetism in exfoliated* VI_3 *layers with magneto-transport*, Nano Lett. **22**, 6149 (2022).

[35] A. Louisy, G. Ouvrard, D. M. Schleich, and R. Brec, *Physical properties and lithium intercalates of* $CrPS_4$, Solid State Commun. **28**, 61 (1978).

[36] Q. L. Pei, X. Luo, G. T. Lin, J. Y. Song, L. Hu, Y. M. Zou, L. Yu, W. Tong, W. H. Song, W. J. Lu, and Y. P. Sun, *Spin dynamics, electronic, and thermal transport properties of two-dimensional* $CrPS_4$ *single crystal*, J. Appl. Phys. **119**, 043902 (2016).

[37] H. L. Zhuang and J. Zhou, *Density functional theory study of bulk and single-layer magnetic semiconductor* $CrPS_4$, Phys. Rev. B **94**, 195307 (2016).

[38] Y. Peng, S. Ding, M. Cheng, Q. Hu, J. Yang, F. Wang, M. Xue, Z. Liu, Z. Lin, M. Avdeev, Y. Hou, W. Yang, Y. Zheng, and J. Yang, *Magnetic structure and metamagnetic transitions in the van der Waals antiferromagnet* $CrPS_4$, Adv. Mater. **32**, 2001200 (2020).

[39] P. Gu, Q. Tan, Y. Wan, Z. Li, Y. Peng, J. Lai, J. Ma, X. Yao, S. Yang, K. Yuan, D. Sun, B. Peng, J. Zhang, and Y. Ye, *Photoluminescent quantum interference in a van der Waals*

magnet preserved by symmetry breaking, ACS Nano **14**, 1003 (2020).

[40] S. Calder, A. V. Haglund, Y. Liu, D. M. Pajerowski, H. B. Cao, T. J. Williams, V. O. Garlea, and D. Mandrus, *Magnetic structure and exchange interactions in the layered semiconductor* $CrPS_4$, Phys. Rev. B **102**, 024408 (2020).

[41] J. Deng, J. Guo, H. Hosono, T. Ying, and X. Chen, *Two-dimensional bipolar ferromagnetic semiconductors from layered antiferromagnets*, Phys. Rev. Mater. **5**, 034005 (2021).

[42] F. Wu, M. Gibertini, K. Watanabe, T. Taniguchi, I. Gutiérrez-Lezama, N. Ubrig, and A. F. Morpurgo, *Gate-controlled magnetotransport and electrostatic modulation of magnetism in 2D magnetic semiconductor* $CrPS_4$, Adv. Mater. **35**, 2211653 (2023).

[43] F. Wu, M. Gibertini, K. Watanabe, T. Taniguchi, I. Gutiérrez-Lezama, N. Ubrig, and A. F. Morpurgo, *Magnetism-induced band-edge shift as the mechanism for magnetoconductance in* $CrPS_4$ *transistors*, Nano Lett. **23**, 8140 (2023).

[44] M. Huang, J. C. Green, J. Zhou, V. Williams, S. Li, H. Lu, D. Djugba, H. Wang, B. Flebus, N. Ni, and C. R. Du, *Layer-dependent magnetism and spin fluctuations in atomically thin van der Waals magnet* $CrPS_4$, Nano Lett. **23**, 8099 (2023).

[45] L. Wang, I. Meric, P. Y. Huang, Q. Gao, Y. Gao, H. Tran, T. Taniguchi, K. Watanabe, L. M. Campos, D. A. Muller, J. Guo, P. Kim, J. Hone, K. L. Shepard, and C. R. Dean, *One-dimensional electrical contact to a two-dimensional material*, Science **342**, 614 (2013).

[46] See Supplemental Material at http://link.aps.org/supplemental/10.1103/PhysRevX.15.011017 for device fabrication and measurement configuration, position of the Fermi level in $CrPS_4$ multilayers, signatures of SCLC in additional $CrPS_4$ devices, comparison of magnetotransport measured under an out-of-plane and in-plane magnetic field, systematic behavior of V_{TF}.

[47] H. H. Kim, B. Yang, S. Tian, C. Li, G.-X. Miao, H. Lei, and A. W. Tsen, *Tailored tunnel magnetoresistance response in three ultrathin chromium trihalides*, Nano Lett. **19**, 5739 (2019).

[48] A. Rose, *Space-charge-limited currents in solids*, Phys. Rev. **97**, 1538 (1955).

[49] M. A. Lampert, *Simplified theory of space-charge-limited currents in an insulator with traps*, Phys. Rev. **103**, 1648 (1956).

[50] B. I. Shklovskii and A. L. Efros, *Electronic Properties of Doped Semiconductors* (Springer Science & Business Media, New York, 2013), Vol. 45.

[51] F. Yao *et al.* (unpublished).

[52] R. H. Fowler and L. Nordheim, *Electron emission in intense electric fields*, Proc. R. Soc. A **119**, 173 (1928).

[53] M. Lenzlinger and E. Snow, *Fowler-Nordheim tunneling into thermally grown* SiO_2, J. Appl. Phys. **40**, 278 (1969).